Accounting for the Varying Supply of Solar Energy when Designing Wireless Access Networks

Margot Deruyck, Daniela Renga, Michela Meo, Luc Martens, and Wout Joseph

Abstract

Traditionally we highly rely on fossil fuels for our energy provisioning, but there are drawbacks on using these fossil fuels: the risk for depletion in the future; the increased in cost as already observed during the last few years, and the high impact on the climate change. One virtually carbon-neutral alternative to fossil fuels are renewable energy sources, like solar energy. In this paper, we investigate the energy and network performance of a wireless access network powered by the traditional electricity grid and a PV (PhotoVoltaic) panel system. An energy-aware management system for the future wireless access networks is proposed. This system consists of the management of the energy provisioning and storage system and the application of the proposed energy-saving strategies which aim to reduce the energy footprint through the traditional grid in case a renewable energy shortage occurs. To evaluate the network's performance, this paper proposes a deployment tool with the above described energy-aware management system. The results show that it is promising to further investigate a more evolved and complex energy-aware management system.

Index Terms

deployment tool, power consumption, prediction model, PV panel, renewable energy sources, solar energy, traditional electricity grid, wireless access network.

I. Introduction

Traditionally, most of the energy we use today comes from fossil fuels. Oil (petroleum), coal, and natural gas made up 82 percent of the world's primary energy supply in 2012, and 68 percent of electricity was generated by burning fossil fuels [1]. However, using fossil fuels has some drawbacks. First of all, they are not renewable. This means that in the future we will have a possible depletion if we continue to use them like we do today. Some scientists argue that current trends in fossil fuel consumption will result in a peak of conventional oil production

M. Deruyck, L. Martens, and W. Joseph are with the Department of Information Technology, Ghent University/IMEC - WAVES, Technologiepark-Zwijnaarde 15, B-9052 Ghent, Belgium e-mail: margot.deruyck@ugent.be

D. Renga and M. Meo are with the Dipartimento di Elettronica e Telecommunicazioni, Politecnico di Torino, Corso Duca degli Abruzzi 24, 10129 Torino, Italy.

Manuscript received

before 2030, leading to a global fuel shortage and a steep increase in oil prices [1]. Whether this depletion will indeed occur is a contested point in literature, but even adversaries of this theory agree that political instability in oil-producing countries can result in severe oil price shocks, with devasting effects for fossil fuel-based economies. Today, we already noticed a significant increase in energy cost. Besides the possible future depletion and the increasing energy cost, burning fossil fuels also have an impact on the climate change. Renewable energy sources offer one of the new virtually carbon-neutral alternatives to fossil fuels.

Wireless access networks are large power consumers. Up to 80% of the energy consumption in 3G and LTE (Long Term Evolution) mobile networks is caused by the base stations [2]. The first studies of powering these base stations with renewable energy sources (i.e., with solar and wind energy) start to appear in literature [4], [5], [6], [7], [8]. The main driver to use renewables for mobile networks was first given by dealing with the absence or unreliability of the traditional electricity grid when deploying mobile networks in remote areas. However, due to the increased awareness of the general public and the policy makers about the drawbacks of burning fossil fuels, current research strongly aims at investigating the promising role of renewable energy in mobile networks for reducing the grid energy consumption and thus the electricity costs. Furthermore, in the future, the mobile network will become part of the smart grid. The smart grid will possibly be largely off-grid with renewables as only energy sources [9]. The different parts of the smart grid will have to align their energy need on each other [10] since renewable energy sources will not provide the same supply continuity as currently been offered by fossil fuels because of the varying weather conditions. From this point of view, it is important to investigate the integration of an energy-aware management of radio resources within the mobile network. Only few recent works have considered energy-aware management in order to reduce the grid energy consumption and complying with the typically intermittent availability of renewable energy [11], [12]. Furthermore, Resource on Demand (RoD) strategies are becoming popular as effective solutions to dynamically adapt the energy consumption of the mobile access network to the varying traffic demand. Indeed, the base station's power consumption is very little traffic proportional and even during off-peak periods their overall consumption can be reduced by only 20-40% at most [3]. RoD strategies allow to save energy by switching off some of the radio resources during periods of time in which they are not needed. Nevertheless, not many studies investigate the impact of RoD approaches exploiting BS sleep modes combined with the use of renewable energy to power base stations, along with energy harvesting techniques to tackle the intermittent nature of renewable energy production, in terms of energy efficiency, power outage risk and overall mobile network performance [13], [14], [15], [16], [17], [18]. [14] considers a cellular network where some base stations are powered by renewable energy only, while other base stations are only connected to the traditional power grid. Based on dynamic programming, an optimal BS sleep policy is obtained, according to energy and traffic variation, in order to save energy and, for renewable powered base stations, harvest energy for future usage. A simpler heuristic algorithm is also proposed, that defines the number of active renewable powered base stations based on network traffic, while the deactivation of grid powered base stations is left to a dynamic programming algorithm. In [15], authors consider cloud based heterogeneous cellular networks with hybrid energy sources. An optimization problem is formulated to reduce the energy consumption from the grid and balance the loads among base stations. A centralized algorithm for BS operation and user association is then proposed, exploiting the cloud platform calculating power. [16] investigates a

portion of a mobile access network where base stations, equipped with photovoltaic panels and an energy storage, can be powered either by solar energy or by the power grid. Real location based data about traffic and solar irradiation are considered. A base station switching on/off policy operates in a centralized way to reduce energy consumption, taking the decision depending on the actual traffic load and guaranteeing a minimum capacity for satisfying current user demand. Optimal system dimensioning is investigated and operational costs are taken into consideration by evaluating the energy bill reduction, while CAPEX cost for PV system and batteries are also analyzed. In [17], authors study the problem of energy efficiency in cellular heterogeneous networks using radio resource and power management combined with a BS switching on/off approach. The developed framework also incorporates the availability of locally generated renewable energy and it is employed to provide an efficient use of the radio resources and a minimization of the energy consumption. Two methods are proposed, providing an optimal and near optimal solution to the problem. The authors in [18] model a mobile network powered by hybrid energy sources, where a radio resource and energy management policy is applied to minimize costs. Our work rather aims at proposing and comparing various resource management strategies applied to a green mobile network to reduce the amount of energy bought from the grid during a critical period in wintertime, which represents a worst-case period, since the irradiation and, consequently, the levels of renewable energy production are low. Unlike [18], our work investigates a realistic scenario, deployed by means of the tool proposed in [19], considering an existing suburban area of 0.3 km^2 with traffic of residential type and uniform distribution of the users. Moreover, our paper studies a heterogeneous network where macrocell and microcell base stations coexist, and their locations are distributed according to the actual installations placed in the considered area. In [18], simulations are performed over a period of one day, assuming 24 time horizons of one hour each. In our work, the simulation period is longer, covering an entire week, hence being more representative of a real system operation, due to the higher variability observed in terms of renewable energy generation levels and base station consumption over time. Moreover, more than one strategy to switch base stations on/off and for energy management are proposed and compared. Furthermore, in [18] a time granularity of one hour time steps is considered. Conversely our work, besides strategies simply operating on an hourly basis, proposes additional strategies where the decisions about activating/deactivating base stations and about energy management are taken also based on the prediction about future renewable energy shortages that may occur during a time window lasting from 1 to 10 hours. Finally, the results obtained from our simulations are used to deploy analytical prediction models, that are useful tools for achieving a proper dimensioning of the energy provisioning and storage system in a real mobile network setup.

In this paper, we investigate the energy and network performance of a wireless access network powered by the traditional electricity grid and a PV (PhotoVoltaic) panel system. An energy-aware management system for the future wireless access networks is proposed. This system consists of the management of the energy provisioning and storage system and the application of energy-saving strategies, which aim to reduce the amount of energy that should be bought from the traditional grid in case a renewable energy shortage occurs. The decision taken by these strategies considers the actual power demand, based on the level of available renewable energy that is currently produced or has been previously harvested, which is a novel approach. To evaluate the network's performance, this paper proposes a deployment tool including the above described energy-aware management system. To the

best of the authors' knowledge, such a deployment tool has never been proposed before. Furthermore, the use of energy-aware strategies in wireless access networks paves the way for the proposal of new approaches that combine radio resource management and energy generation. These approaches are strategic in new challenging contexts such as the smart grids, in which demand-response mechanisms require to dynamically adapt the energy demand to the smart grid requests. Furthermore, they have also to cope with power grid instabilities and outages, as in the case of emerging countries. Finally, we developed different prediction models for the network performance as a function of the energy storage and provisioning system. These novel models allow to properly design the energy system for future wireless access networks.

The outline of the paper is as follows. In Section II, the methodology is discussed. In this section, the considered scenario and energy-aware strategies are proposed. Furthermore, we will discuss the assumptions made for the different parameters of the energy production and storage system. Finally, we will focus on how the deployment tool accounts for the solar energy predictions and which network and energy performance metrics are considered. Section III presents the results obtained with the deployment tool and compares the performance of the three strategies based on the proposed metrics. A thorough analysis of the different parameters of the energy production and storage system is performed. Moreover, predictions models for the energy and network performance parameters as a function of the PV panel size, the storage size, and the time window (individually and jointly) are proposed for the considered strategies. We will end this section with guidelines for the most optimal settings of the energy provisioning system when developing future energy-aware wireless access networks. In Section IV, we summarize the most important conclusions from this study.

II. Methodology

A. Scenario

As depicted in Fig. 1, the scenario considered in the paper consists of a group of base stations powered with solar panels and equipped with batteries. The energy generated by the panels is first used to power the BSs and, in case of extra production, is fed into the batteries, according to a first-use-then-harvest principle. Whenever no renewable energy is currently available, the base stations drain energy from the batteries for their supply. In case batteries are discharged, the base stations can be supplied by the power grid. We assume that the renewable energy generator system is shared among the base stations of the group and energy management decisions are taken in a centralized way for the whole group of base stations. This means that decisions are based on the total available energy and the total power demand regardless the actual implementation of the power system that, in its turn, can either be distributed, with small solar panels and storage units co-located with the base stations, or composed of a few larger generators.

In terms of energy generation, a worst case scenario is considered: the winter period of 3 January till 9 January (i.e., 1 week) for the area of Turin, Italy. To predict the energy production by the PV panels, the data from [20] is used. The adopted traces reports data, provided on an hourly basis, about the power output obtained per each kWp of nominal capacity of the PV panel system. The values of renewable energy production are derived based on real data of solar irradiation in the city of Turin observed in the corresponding week of January during the

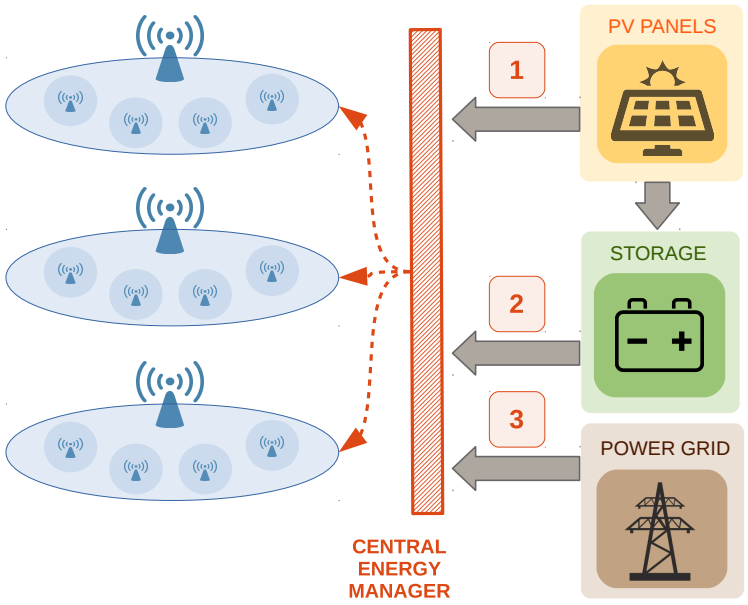

Fig. 1. Scenario with the mobile access network powered by RE energy and by the traditional power grid. In order to ower the BSs, priority is given first to PV panels (1), then to the energy previously harvested in the storage (2) and finally to the electric power grid (3).

Typical Metereological Year. Energy losses due to the efficiency of PV modules and to the normal PV system operation are taken into account. For energy harvesting, lead-acid batteries represent a common technology adopted in renewable energy systems. A set of lead-acid battery units, each with capacity of 200 Ah and voltage 12 V, is hence assumed as storage in this work. The simulations are performed for a time frame of 1h for a typical suburban environment as shown in Fig. 2(a). In this area, 8 macrocell base stations are located (indicated by the dark blue large squares), each supporting 4 microcell base stations (represented as light blue small squares). The locations of the macrocell base stations in Fig. 2(a) are the locations from the macrocell base stations in a real network from an mobile operator active in the area. The microcell base stations are indeed regularly generated from the macrocell base station. As the user traffic varies during the simulation period, we chose to show here the user locations (as green circles) during the 5 p.m. time slots as an example. The support is limited to 4 microcell base stations per macrocell base station to avoid an over-dimensioned network for the considered amount of traffic. To model the user traffic, realistic data from an operator is considered as proposed in [21]. Fig. 2(b) shows how the number of active users vary during one week. For the user bit rate requirements, two bit rates are proposed: 64 kbps for voice calls and 1 Mbps for data calls. The users are assumed to be uniformly distributed over the area since a limited area of 0.3 km^2 consisting of only residential houses. There are no hotspots such as touristic attractions or parks present in the area. This means that each location has the same chance to be chosen as possible location for the user. All information about the buildings in the environment is delivered in the form of a shape file.

Furthermore, LTE Advanced is considered as wireless technology at a frequency of 2.6 GHz. Table I lists all the relevant link budget parameters for the assumed scenario [22]. The power consumption of the macrocell and

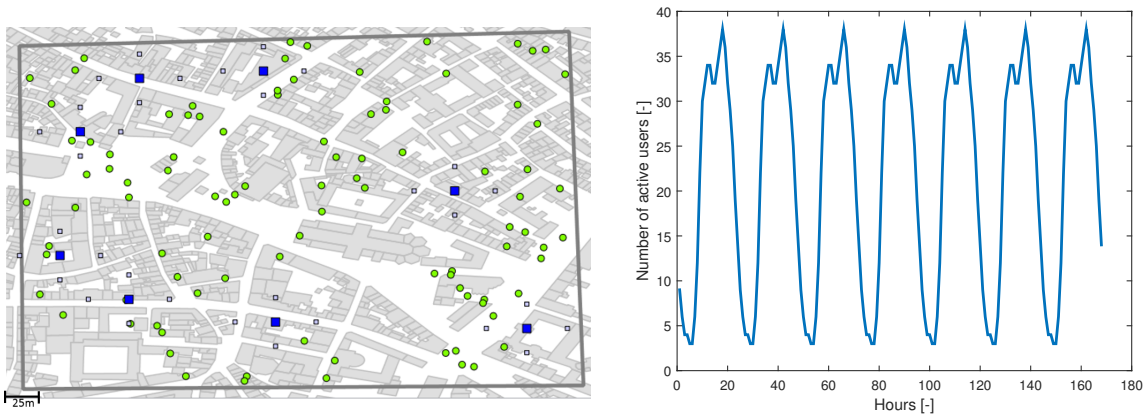

(a) (b)

Fig. 2. The considered suburban area of 0.3 km^2 (a) with the base station (dark blue large square = macrocell base station, light blue small square = microcell base station) and user locations (green circles) for the 5 p.m. time slot and the evolution of the number of active users (b) during one week [21].

microcell base stations is modelled as proposed in [22]. It is assumed that during sleep mode, the base station does not consume any power.

B. Strategies

As mentioned above, different energy-aware strategies will be considered in case of a renewable energy shortage.

Several studies are available in the literature where various base station management strategies are proposed, in which base stations are switched on or off depending on the current users demand. An extensive review of radio resource management techniques can be found in [23], [24]. These strategies, despite being simple, are widely shown to be effective in saving energy, still mantaining an acceptable level of end user experience. The decision of putting into sleep mode microcell base stations rather than the macro cell base stations is due to the fact that the macrocell base stations are responsible of the baseline coverage in their relevance area, whereas the microcell base stations provide additional capacity for peak time, rather than extended coverage. Hence, mobile network operators will hardly take a significant risk of capacity holes and poor service quality for their customers, by switching off a macrocell base station and relying only on microcell base stations. The criterion of first switching off the least loaded BSs is adopted also in other studies [16], where the resource on demand strategy dynamically adapts the number of radio resources to the actual traffic load, by switching off one or more microcells base stations. The decision is taken according to a load proportional criterion, since the base stations handling the lowest traffic loads are turned off and their traffic moved to a neighbouring macrocell base station. In the current work, the decision is taken by putting into sleep mode the least loaded microcell base stations in terms of number of users.

The following strategies are proposed:

1) ‘No action’: when using this strategy no adjustments will be made on the network level. We just buy the needed amount of energy from the traditional electricity grid, while keeping the network fully operational.

TABLE I

LINK BUDGET PARAMETERS FOR THE LTE-A MACROCELL AND MICROCELL BASE STATION [22].

Parameter	Macrocell base station	Microcell base station
Frequency	2.6 GHz	
Maximum input power antenna	43 dBm	33 dBm
Antenna gain base station	18 dBi	4 dBi
Antenna gain mobile station	2 dBi	
Soft hand over gain	0 dB	
Feeder loss base station	0 dB	0 dB
Feeder loss mobile station	0 dB	
Fade margin	10 dB	
Yearly availability	99.995%	
Cell interference margin	0 dB	
Bandwidth	5 MHz	
Receiver SNR	1/3 QPSK = -1.5 dB, 1/2 QPSK = 3 dB 2/3 QPSK = 10.5 dB, 1/2 16-QAM = 14 dB 2/3 16-QAM = 19 dB, 4/5 16-QAM = 23 dB 2/3 64-QAM = 29.4 dB	
Used subcarriers	301	
Total subcarriers	512	
Noise figure mobile station	8 dB	
Implementation loss mobile station	0 dB	
Height mobile station	1.5 m	
Coverage requirement	90%	
Shadowing margin	13.2 dB	
Building penetration loss	8.1 dB	

Studying this strategy is important since it is representative for the current situation. It is considered as the reference scenario and we will refer to it as the fully operational network.

2) 'All microcell base stations off': when this strategy is applied, all microcell base stations will be turned off when the local available energy (renewable energy produced and stored) is not enough to power the base stations. The decision is taken based on the network's energy demand, the energy stored on the battery and the energy generation in a time frame. All users connected to these microcell base stations need to be reconnected to a macrocell base station to the best extent possible. It might occur that there is still not enough renewable energy available, even when all microcell base stations are switched off. Whenever this is the case, we will buy the energy from the traditional grid to keep at least the macrocell base stations up and running. In case that there is any extra amount of renewable energy left over when the microcell base stations are switched off, this amount of renewable energy is harvested in the battery for future usage.
3) '1 to 4 microcell base stations off': the final strategy is a hybrid one. Microcell base stations will be turned off in the event of an energy shortage, but will be switched off gradually. First, we determine how many renewable energy is available compared to the energy consumed by the fully operational network. Next,

we calculate the network's energy consumption when switching off 1, 2, or 3 microcell base stations per macrocell base stations. As soon as the network's consumption becomes lower than the amount of available renewable energy, we know how many microcell base stations we have to turn off per macrocell base station. If turning off 3 microcell base stations is not sufficient, the second strategy will be applied. Similar to second strategy, we need to reconnect all the users connected to the sleeping microcell base stations to the best extent possible. In case that there is any extra amount of renewable energy left over when the microcell base stations are switched off, this amount of renewable energy is harvested in the battery for future usage. The order in which the microcell base stations are turned off is based on the number of users served by the base station. The microcell base station serving the lowest number of users is switched off first.

The last two strategies will be combined with a prediction time window t (in hours). Fig. 3 introduces this time window. Without considering a time window, we determine the network's energy demand and energy production for a certain time frame or time stamp, which will be every 1h for this study. When a renewable energy shortage is predicted for this time stamp, we can apply one of two strategies mentioned above. The procedure to identify a renewable energy shortage at a certain time stamp TS is as follows:

1) Determine the power consumption of the network at time stamp TS before any action is been taken. Note that the power consumption of the network will vary from time stamp to time stamp due to the varying user traffic as will be discussed in Section II-D.
2) Determine the energy produced by the PV panel system at time stamp TS. The data from the PVWatts tool provides us on an hourly basis the output power produced per kWp nominal capacity of the PV panel system. This output power is multiplied by the assumed nominal capacity of the considered PV panel system.
3) If the sum of the amount of produced energy by the PV panel system and the amount of energy stored at the battery at time stamp TS is lower than the network's power consumption, we conclude that a renewable energy shortage will occur. Note that it depends on the number of users, their locations, and bit rate requirements how many base stations are active.

When considering a time window, we also account for an energy shortage in the next few hours. For example, assuming a time stamp TS and a time window of 10h. If we predict an energy shortage between TS and $TS + 10$ (boundaries included), microcell base stations will be switched off from TS on. When combining the third strategy with a time window, we consider the network's power consumption at the first time stamp between TS and $TS + 10$ for which an energy shortage occurs. Based on the amount of renewable energy that is needed, we can calculate how many microcell base stations have to be switched off and apply this to the network of time stamp TS. If a higher number of microcell base stations has to be turned off than available at time stamp TS, all microcell base stations will be switched off.

In relation to the accuracy of the prediction of a renewable energy shortage occurrence, first we consider the forecast consumption. The network consumption prediction can be sufficiently accurate, since the traffic patterns tend to be repetitive and rather predictable from day to day [25]. Furthermore, the base station consumption is very little traffic proportional, hence small shifts of the actual traffic load with respect to the predicted pattern would have a

limited impact on the consumption [3]. Secondly, in relation to the forecast of future renewable energy production, the data about renewable energy production obtained from PVWatts are derived from the analysis of huge datasets, covering many years. The values of renewable energy production provided by this tool for the period of one year should hence be interpreted as a representative estimate for a real photovoltaic system, operating in a year with the typical weather variations observed in the location where the system is installed. Of course, there is a certain variability in the actual weather conditions observed during the same months and days across different years. Hence, the PVWatts values of the total yearly and monthly energy production, derived from weather data representing long-term historical typical conditions, may indeed show errors as high as ±10% and ±30%, respectively, with respect to the real production related to a specific year [26]. However, in our study, we simply select a sample period in the year in which the production is low and over which the simulations are run, considering a sample pattern of renewable energy production that is realistic and representative of the location based typical meteorological conditions and avoid extreme condition scenarios.

According to the literature there may be huge variability in the total daily solar irradiation, hence in the energy production level, from day to day [25]. Furthermore, within the same day, there may be a significant variability in the irradiation level, with fast and frequent modifications of sun irradiation within short periods of the order of minutes. It may not result easy to exactly predict these very short term variations, although methods exists to make rather accurate forecasts of these modifications in solar energy production [27]. However, according to the strategy proposed in our work, the predictions of the renewable energy generation refer to the production during rather longer periods of some hours (i.e. the duration of the time window W). Considering this time scale, the prediction of the cumulative amount of renewable energy produced in a period of 1 to 10 hours, based on weather forecast, is sufficiently accurate with negligible error [28], [29], [30], [31], [32]. Indeed, the pattern of the average solar irradiation from hour to hour typically follows a bell shape, whose peak may vary depending on the weather of the specific day, but the shape remains the same [25]. Given the current day weather conditions and the knowledge of short term weather forecast, this pattern can be predicted accurately enough, with a mean relative error of few percentage points even when forecasting the production up to the following day [32].

C. Energy production and storage system

For the energy production, predictions for the period from January 3 until January 9 (1 week) for the area of Turin, Italy will be used [20]. As mentioned above, we assume a worst-case scenario. During this period, it is winter time in Italy and the hours of sunshine per day are very limited.

Besides a connection to the traditional electricity grid, each macrocell base station (each supporting 4 microcell base stations) comes also with a PV panel of 12.5 kWp. As previously mentioned, PV panels might be physically co-located with the base stations or they might be concentrated in a few larger sites that provide power supply for the whole group of base stations. This results in an overall PV panel capacity of 100 kWp. [5], [6], [7] propose a PV panel size between 9.3 and 16.6 kWp (in combination with a proper battery dimensioning) to power a macrocell base station completely. Approximately 4.9 m^2 of space should be reserved per kWp offered by the PV panel system [5]. Based on our assumptions, an area of about 490 m^2 should be allocated for the whole network's panel

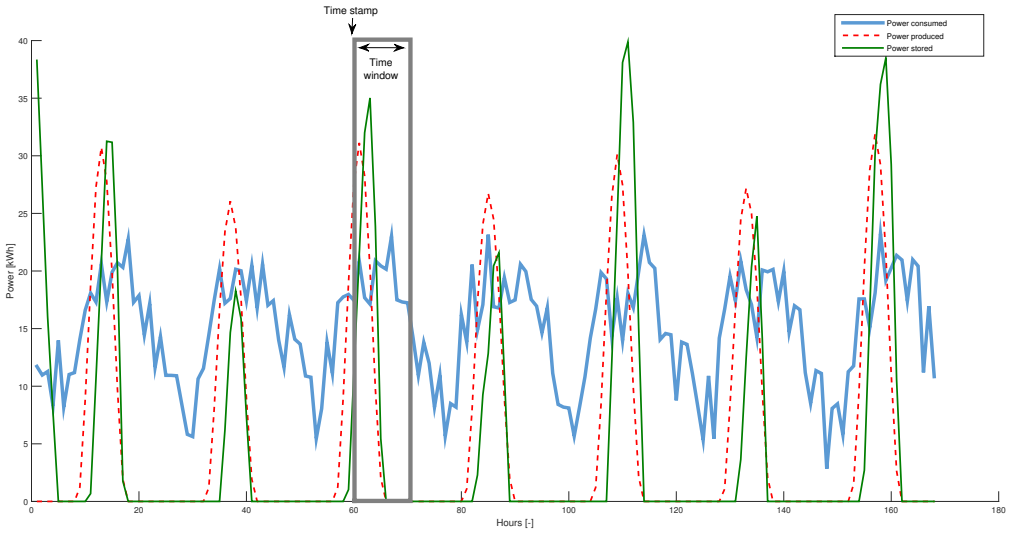

Fig. 3. Time frame versus time window.

system. Note that we assume a distributed energy provisioning and storage system, grouping all PV panels and all bateries in a cluster. Hence, every base station can draw the available stored energy from the battery system without any constraints. To handle the centralized management of this system, a central controller will be available at the cluster. This controller takes also care of the information exchange for proper operation. We neglect any losses occuring during the (dis)charge of the battery and the energy transfer or transmission.

In relation to scalability issues, even in case of a larger network a single controller would be sufficient to run the algorithm over the whole network, since the limited computational complexity to run the implemented strategies does not require significant computational power. In relation to the information exchange in larger networks, no significant delay would be experienced, since the decisions are taken every hour. Finally, in relation to the renewable energy transfer within a larger network area, there might be slightly higher transfer losses due to the larger size of the network. However, even if some energy transfer may occur between different locations of solar energy generators, the renewable energy generators are meant to operate locally. Hence the renewable energy is produced and consumed locally whenever possible and, only when needed, it is transferred among neighbour BSs, avoiding energy transfer over longer distance. The transfer losses would hence be rather limited even in case of larger networks. From the simulator point of view, scalability is also not an issue, since it has been developed in such a way that it can design a network based on a flexible number of possible base station locations. The larger this set, however, the longer the simulation duration. The simulation duration can be further reduced by parallelizing some parts of the algorithm.

Our simulations start on January 3, 12 a.m. We assume that the battery is completely full at the start of the simulations.

D. Deployment tool: accounting for solar energy predictions

To investigate the energy and network performance of the different considered strategies, the capacity deployment tool proposed by [21] is extended. The goal of this tool is to develop a network with a minimal power consumption and/or a minimal exposure for human beings by taking into account the instantaneous bit rate requested by the users active in the area. Although the tool allows to optimize the network towards both power consumption and exposure, we will here focus only on the power consumption optimization. The deployment tool starts from a set of existing macrocell base station locations i.e, 8 locations for the considered scenario (Section II-A). At the starting point, all base stations are in sleep mode. Based on this set, the algorithm determines which macrocell base stations are the most appropriate base station to switch on along with the 4 microcell base stations it is supporting. The other base stations will remain in sleep mode. Based on this set, the algorithm determines which base stations are the most appropriate base station to switch on. The other base stations will remain in sleep mode. Furthermore, the input power of the base station's antenna is fine tuned. When optimizing the network towards power consumption, a network with a low number of high-powered base stations is typically obtained [21]. Due to this, the algorithm tries to connect the users as much as possible to the already active base stations. To do this, the input power of the base station's antenna can be increased when necessary (until a certain predefined level as shown in Table I). However, on the other hand, when it is possible to serve the same user with a lower input power, the input power can be decreased to save some extra energy [22]. The optimization of the network is on an hourly base, so the algorithm described above is repeated for every hour. The tool works thus on the level of the management of the installed base stations in the considered area. In order to account for the solar energy predictions and applying the different strategies, an extended version of the tool is proposed. The flow diagram of the algorithm is shown in Fig. 4.

We will simulate the network for one week on a 1h time frame base. This means that for every hour of the week (Fig. 4 Step 1), we will develop a network for the user traffic representative for that time stamp. If we are considering a certain strategy and a energy shortage is predicted for the current time frame TS, (some of) the microcell base stations from the developed network will be switched off. When considering a time window of T hours, we will also design the networks for the next T hours. In case, an energy shortage is predicted in this next T hours, the microcell base stations from the network developed for time stamp TS will be switched off.

Returning now back to the algorithm, for each time slot, the number of users active in the considered area, their location and their bit rate requirements have to be determined (Step 2) as described in Section II-A. Once all user information is available, the network can be developed (Step 3). The algorithm will try to connect each user to an already active base station (since less power is needed to increase the antenna's input power than waking up a base station). Therefore, the path loss experienced by the user from this base station should be lower than the maximum allowable path loss and the base station should still be able to offer the bit rate required by the user. As mentioned in Section II-A, each user requires a certain bit rate. This bit rate corresponds with a certain modulation scheme and coding rate which corresponds with a certain receiver sensitivity. Based on this receiver sensitivity and the link budget parameters of Table I, one can determine how much path loss the user might experience but still be

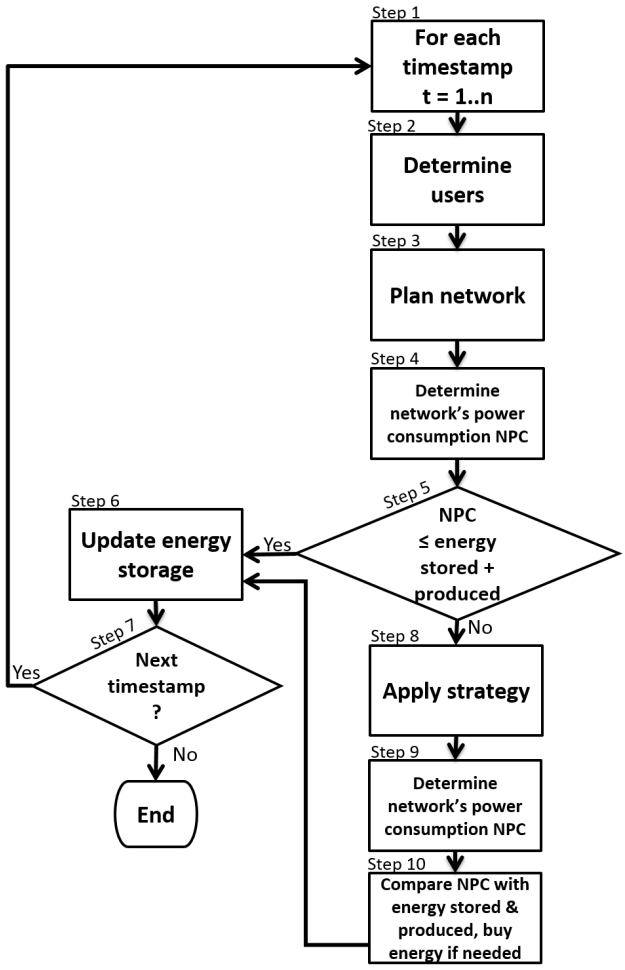

Fig. 4. Flow diagram of the algorithm.

able to decode the received signal. If the experienced path loss is lower than this maximum allowable path loss, the user will be served with its assigned bit rate. However, this does not mean that the base station can still offer this bit rate as the base station is most likely also serving other users. To this end, the maximum capacity that can be offered by the base station is determined and the algorithm keeps track of how much is already spent by the other users. Furthermore, an extra check on the number of served users is performed by using the approach described in [33]. If it is not possible to connect a user to an already active base station, one of the sleeping base stations will be switched on, if possible. If a sleeping base station is turned on, the algorithm tries to reconnect already covered users but only when they are experiencing a lower path loss than from the base station they were connected to. In this way, the load is spread over the whole network. When a macrocell base station is switched on, we also switch on the 4 microcell base stations supported by this macrocell base station. Note that a user can only connect to a microcell base station when the macrocell base station is already switched on. Once the network is developed, its power consumption NPC (Network's Power Consumption) is calculated (Step 4) based on the models proposed in [22]. This NPC is then compared to the amount of available energy i.e., the amount of energy that is

produced and stored. Whenever the NPC is lower than the available energy, no strategy needs to be applied and only the energy storage needs to be updated (Step 6). Otherwise, one of the strategies proposed in Section II-B is applied (Step 8). Since some of the strategies switch off base stations, the network's power consumption needs to be redetermined (Step 9) and compared to the amount of available energy (Step 10). If there is still not enough energy available, we will buy the required amount of energy from the traditional electricity grid in order to keep the (slimmed version of the) network active. In this case, we also need to update the energy storage (Step 6) and proceed to the next time stamp if any still available (Step 7).

Note that the macrocell base stations are switched on when decisions on the network planning level are taken place, not at the level (and time scale) of the strategies. The strategies work only on swichting off the microcell base stations. The study of interactions between the decisions of switching the base stations on/off in different tiers, possibly managed by different mobile operators, has not explicitly considered in this work. However, some centralized coordination policy could be easily envisioned and implemented in order to handle the issue, without significant impact on the obtained results, as long as different mobile operators establish an agreement on this aspect. Indeed, some financial agreements already exist among mobile operators allowing to use their own mobile infrastructures as a unique set of radio resources.

E. Metrics

In the first part of this study, the following metrics are considered for each time frame:

- – Power consumed by the network: This parameter shows how much energy the network is currently consuming.
  - – Power produced by the PV panels: This parameter tells us how much energy is currently produced by the PV panels.
  - – Power stored by the energy storage system: represents how much energy is currently stored by the energy storage system.
  - – Power available for consumption: This parameter shows how much renewable energy is currently available to consume. It equals the power currently produced by the PV panels and the power currently stored by the energy storage system.

In the second part of this study, the influence of different parameters of the energy production and storage system are investigated using the following energy related metrics:

- – Total consumed energy (in Wh) : This parameter describes how much energy (renewable energy and energy bought from the traditional grid) is consumed during the whole simulation period.
  - – Average stored (energy in Wh): This parameter corresponds with the average amount of energy that is stored over the whole simulation period.
  - – Total energy bought (in Wh): This parameter shows us how much energy should be bought from the traditional grid during the whole simulation period. Furthermore, we consider also ΔP, which represents the relative improvement or deterioration ot the total energy bought compared to the reference scenario.

- Time sufficient energy available (as a percentage): this ratio expresses how much of the simulation period the network is operating on renewable energy only and no energy should be bought from the traditional network.

Furthermore, also the influence on the following network performance related metrics will be studied:

- Average geometrical coverage (as percentage): This metric represents how much percent of the considered area is covered on average by the developed networks over the whole simulation period.
- Average user coverage (as percentage): tells us how many users on average are covered by the developed networks over the whole simulation period. Also the relative difference ΔU in average user coverage compared to the reference scenario will be considered.
- Average network capacity (in Mbps): shows how much capacity is offered by the developed networks on average over the whole simulation period. Furthermore, the relative increase or decrease ΔC in average network capacity compared to the reference scenario will be considered.

III. Results

A. Evolution of the energy consumption, production, and storage during the week

In this section, we investigate how the power consumed by the network, the power produced by the PV panels, the power stored by the energy storage system, and the power available for power consumption evolves during one week. As mentioned above, a worst case scenario is assumed i.e., one week during the month of January. Figs. 5(a), 5(b), and 5(c) show the evolution of the considered metrics when taking no action at all (Strategy 1), turning off all microcell base stations (Strategy 2), and switching off 1 to 4 microcell base stations (Strategy 3), respectively.

The blue full line in Fig. 5 shows the energy consumption of the network during the whole week. The network's power consumption clearly follows the trend line of the number of active users of Fig. 2(b). For the three strategies, the highest power consumption is daily obtained around 5 p.m. (hours 17, 41, 65, etc. with a power consumption of approximately 23.2 kWh) and the lowest power consumption during the night i.e., around 4 a.m (hours 4, 28, 52, etc. with a power consumption of 2.8 kWh when taking no action and around 2.5 kWh when switching off all or 1 to 4 microcell base stations). The study of [34] confirms that the network's power consumption is related to the number of active users.

The evolution of the energy produced by the PV panels during the whole week is shown by the dashed orange line in Fig. 5. Similar results are obtained for the three strategies as the same PV panel system is considered. A peak is reached daily around 1 p.m. (as then most sunshine; between 26 kWh and 32 kWh produced depending on the considered day). Furthermore, between 6 p.m. and 8 a.m. no energy is produced at all (night). This is due to the worst-case scenario we considered so the hours where energy is produced are limited. In January, the sunset is between 8 a.m. and 9 a.m., while the sundown is around 6 p.m. Between sundown and sunset, it will of course not be possible to produce solar energy.

The grey full line in Fig. 5 represents the state of the energy storage system. When more energy is produced than actually consumed i.e., when the orange line in Fig. 5 is above the blue line, the battery is charged. This happens daily around noon. Otherwise, the battery is drained, which is the case between 6 p.m. and 8 a.m. No

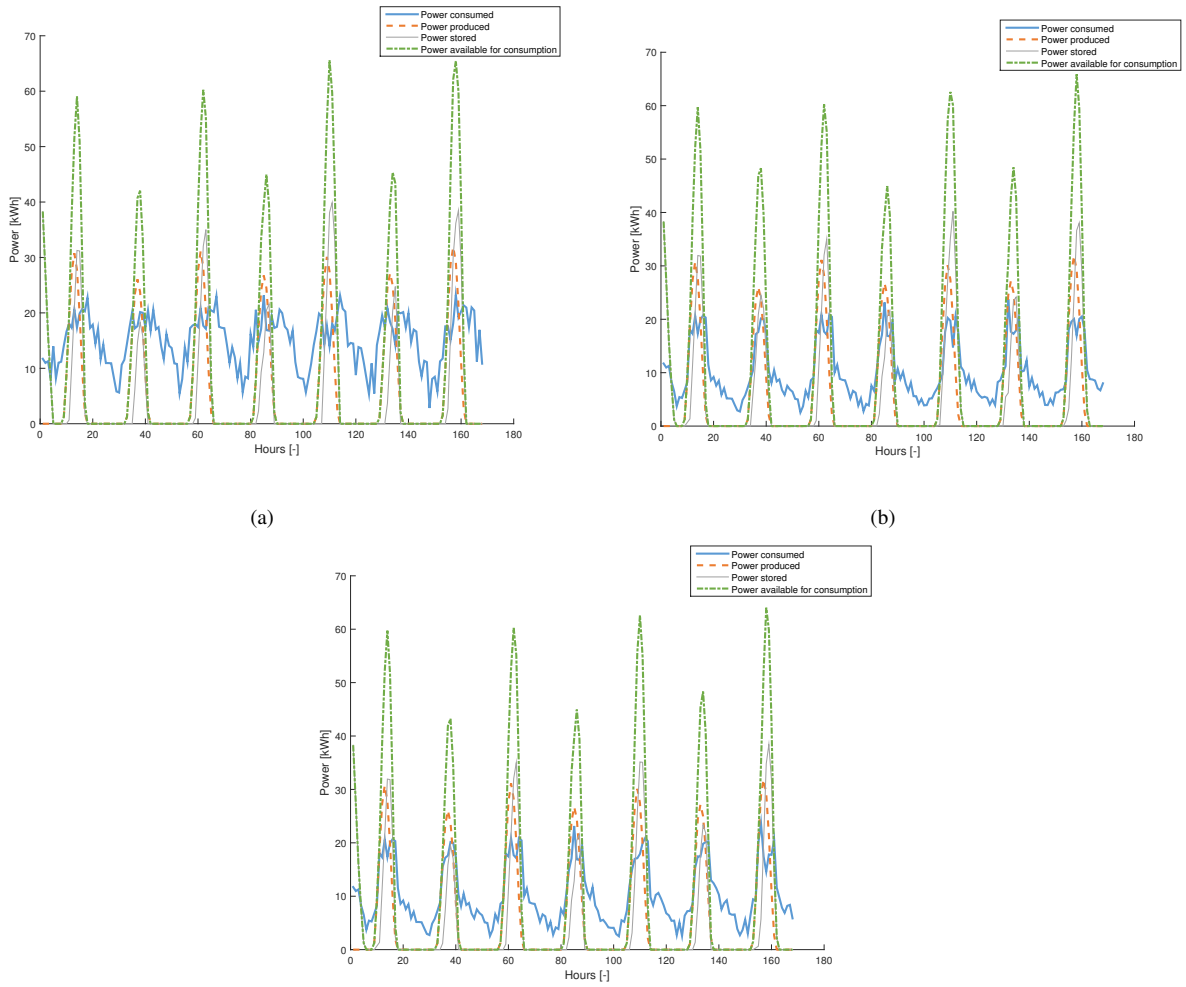

Fig. 5. Evolution of the network's energy consumption, the renewable energy production by the PV panel system, and the energy shortage during one week (168 hours) for the 3 considered strategies: no action (a), all microcell base stations off (b), and 1 to 4 microcell base stations off (c).

significant difference in the amount of stored energy is found between the different strategies. Indeed, the goal of the considered strategies is to reduce the amount of energy that is bought in case of a renewable energy shortage. Furthermore, no time window is here considered, so no energy will be saved in advance for future energy shortages. The influence of a time window on the results will be discussed later. Note also that the energy storage (50 kWh) is never overflowed.

Finally the green dashed-dotted line in Fig. 5 shows the amount of (renewable) energy that is available for consumption. As long as more energy is available consumed by the network i.e., when the green line is above the blue line in Fig. 5, no energy should be bought. For the considered scenario, energy should be bought during the evening and the night. The amount of energy that should be bought, depends on the network's power consumption. Less energy should be bought when applying a strategy to switch off microcell base stations. During the daytime,

all strategies have the same network's power consumption as there is enough energy available as shown in Fig. 5. The difference in the network's power consumption and the amount of energy bought as well as the network performance of the different strategies will be further discussed in detail in the following sections.

B. Influence of the capacity PV modules on the energy and network performance

The influence of the capacity of the PV modules will now be investigated. For this study, the following settings are assumed for the different parameters of the energy system:

- – Capacity of the PV modules: varying from 70 kWp to 200 kWp in steps of 10 kWp
  – Capacity of energy storage: 50 kWh, full at the start of the algorithm
  – Time window: 1h

All other parameters remain the same as mentioned in Section II-A. The influence of the capacity of the PV modules will be evaluated for three different metrics: the amount of bought energy, the user coverage, and the capacity offered by the network.

Table II gives an overview of the absolute and relative values of the different parameters describing the network and energy performance for four different capacities of the PV modules (80, 120, 160, and 200 kWp). The influence of the PV module capacity on the different parameters is discussed in the following sections.

TABLE II
ENERGY AND NETWORK PERFORMANCE OF THE DIFFERENT STRATEGIES WHEN VARYING THE CAPACITY OF THE PV MODULES.

		Energy performance				Network performance				
Capacity PV module [kWp]	Strategy	Total energy consumed [kWh]	Total energy bought [kWh]	Time sufficient energy [%]	ΔP [%]	Average geometrical coverage [%]	Average user coverage [%]	Average network capacity [Mbps]	ΔU [%]	ΔC [%]
80	1: No action	2584	1803	18.5	—	85.4	97.4	455	—	—
	2: All off	1596	825	21.4	-54.2	85.1	94.4	181	-3.1	-60.3
	3: 1 to 4 off	1600	819	19.6	-54.6	85.3	94.1	185	-3.4	-59.3
120	1: No action	2544	1493	32.7	—	85.8	97.3	447	—	—
	2: All off	1791	758	35.1	-49.3	85.2	95.6	239	-1.7	-46.4
	3: 1 to 4 off	1825	770	33.9	-48.4	85.1	95.2	242	-2.2	-45.8
160	1: No action	2564	1425	36.3	—	85.4	97.1	451	—	—
	2: All off	1821	686	36.3	-51.9	84.6	95.2	247	-2.0	-45.2
	3: 1 to 4 off	1837	698	35.7	-51.1	85.6	95.6	251	-1.5	-44.3
200	1: No action	2545	1352	38.7	—	85.9	97.2	448	—	—
	2: All off	1846	638	37.5	-52.8	85.7	95.4	253	-1.9	-43.6
	3: 1 to 4 off	1905	698	38.1	-48.4	85.7	95.8	266	-1.4	-40.5

1) Energy bought: Fig. 6(a) compares the amount of energy that should be bought for the three considered strategies while varying the capacity of the PV modules. The results clearly show that when no action is taken at all (strategy 1), much more energy should be bought. For example, when considering a capacity of 80 kWp, 1803 kWh

of energy has to be bought, while in the case that all the microcell base stations are turned off (strategy 2) only 825 kWh is bought. When switching off 1 to 4 microcell base stations (strategy 3), only 819 kWh has to be bought (Table II) . In general, when applying strategy 2, 49% to 56% (depending on the capacity of the PV modules) less energy should be bought. For strategy 3, a reduction of 48% to 55% is obtained. This improvement is slightly lower than switching off all microcell base stations because the idea of this strategy is to limit the effect on the network's performance during an energy shortage by keeping as much microcell base stations active as possible. Due to this, less energy is saved for future energy shortages as can be seen from the 'Time sufficient energy' parameter in Table II. When turning off all microcell base stations, there is sufficient (renewable) energy available for 21.4% of the time (assuming 80 kWp capacity). When switching off a relative number of microcell base stations, there is only 19.6% of the time enough renewable energy available.

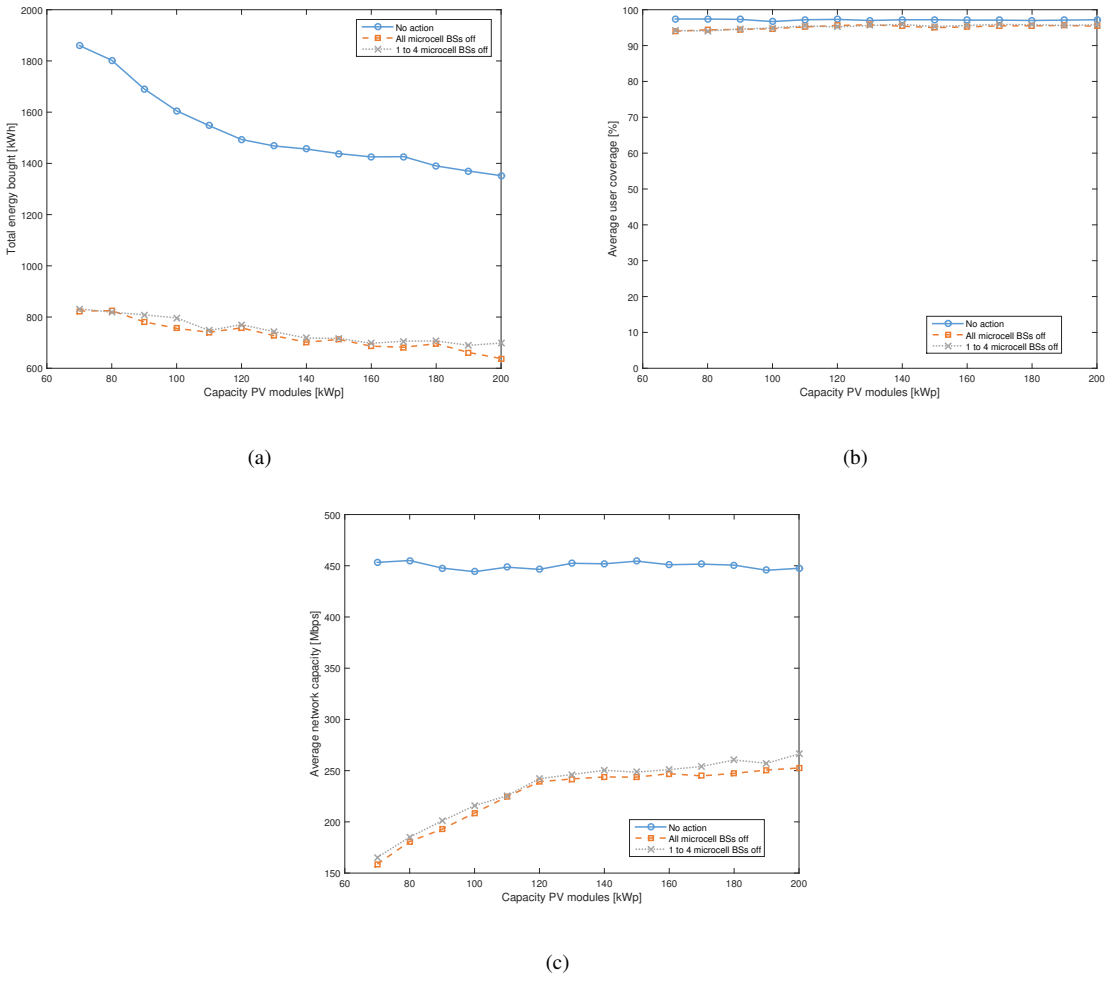

Fig. 6. Comparison of the amount of energy bought (a), the user coverage (b) and the network capacity (c) for the three different strategies as a function of the capacity of the PV modules.

Fig. 6(a) shows also that the amount of energy bought decreases for higher capacity PV modules. When doubling the capacity (e.g., from 80 kWp to 160 kWp), 21.0%, 17.9%, and 14.8% less energy should be bought for strategy

1, 2, and 3, respectively (Table II, from 1803 kWh to 1425 kWh, 825 kWh to 686 kWh, and 819 kWh to 698 kWh, respectively). Note that when we double the PV module capacity, the amount of produced energy doubles (from 788 kWh for 80 kWp to 1576 kWh for 160 kWp). However, the amount of energy bought does not reduce by half due to the fact that the energy storage is not large enough to save all the extra produced energy that is not immediately consumed. Furthermore, when using a PV module capacity of 160 kWp, a total area of 784 m^2 is needed for the PV module itself versus 392 m^2 for 80 kWp [5].

2) User coverage: In Fig. 6(b), the influence of the PV module capacity on the user coverage is shown for the three strategies. A slightly lower user coverage is obtained (about 1.9% to 3.1% for strategy 2 and 1.4% to 3.4% for strategy 3) is obtained compared to the first strategy because all users connected to the sleeping base stations need to be reconnected to the active ones. This is not always possible as the capacity of these base stations might already be used completely. Furthermore, the path loss experienced by the user from these base stations can also be too high. In these cases, the user remains uncovered, resulting in a lower user coverage. The difference in user coverage between strategy 2 and 3 is very limited, since the moments where it is possible to switch off less than 4 microcell base stations are very limited as shown by the total energy consumed parameter in Table II. When considering a PV module capacity of 80 kWp, the total energy consumed amounts to 1596 kWh for strategy 2 versus 1600 kWh for strategy 3 (Table II).

As shown in Fig. 6(b), the capacity of the PV module has not a significant influence on the user coverage. Using strategy 1, the capacity of the PV module has no influence at all on the user coverage since no base stations are switched off. When applying strategy 2 and 3, doubling the PV module capacity increases the user coverage only slightly with 0.8% (94.4% for 80 kWp versus 95.2% for 160 kWp, Table II) and 1.5% (94.1% for 80 kWp versus 95.6% for 160 kWp, Table II), respectively, because we have to turn off the microcell base stations less frequently. For example for strategy 2, there is enough renewable energy available for 21% of the time when assuming a PV module capacity of 80 kWp versus 36.3% when using a capacity of 160 kWp (Table II).

3) Network capacity: The influence of the PV module capacity on the average network capacity is shown in Fig. 6(c). Similar to the user coverage, the PV module capacity has no influence on the network capacity when applying strategy 1. However, applying one of the other strategies has a huge influence on the network capacity as shown by Fig. 6(c). A reduction between 44% to 60% (depending on the considered PV module capacity) is obtained for strategy 2 and between 41% to 59% for strategy 3 compared to the reference scenario (Table II). Furthermore, doubling the capacity from 80 kWp to 160 kWp results in 15% more network capacity (from 45.2% to 60.3% and 44.3% to 59.3% for strategy 2 and 3, respectively, Table II). A higher PV module capacity allows to produce more renewable energy and thus we can keep all base stations active for longer periods (as can be seen by the time sufficient energy parameter in Table II), obtaining a higher network capacity.

C. Influence of the energy storage on the energy and network performance

In this section, we investigate how the energy storage size influences the energy and network performance of the obtained solution. The following settings are assumed for the different parameters of the energy system:

- – Capacity of the PV module: 140 kWp. Note that this is quite large and perhaps unrealistic, as a surface of 686 m^2 will be needed to install the PV modules. However, the purpose of this section is to study the influence of the energy storage size. Therefore, it is important to consider a large enough PV module capacity in order to ensure that the energy storage is not completely loaded and renewable energy is wasted as it can no longer be stored.
  - – Capacity of the energy storage: varying from 30 kWh to 160 kWh in steps of 10 kWh, full at the start of the algorithm
  - – Time window: 1h

All other parameters remain the same as mentioned in Section II-A. The amount of energy bought, the average user coverage, and the average network capacity are again considered as the three key parameters to evaluate and will be discussed in the following sections. Note that the performance of the different strategies for these three parameters is thoroughly compared above and we refer therefore to Section III-B1, III-B2, and III-B3. Table III summarizes the absolute and relative values of the other energy and network performance parameters for four different energy storage sizes (40, 80, 120, and 160 kWh).

TABLE III
ENERGY AND NETWORK PERFORMANCE OF THE DIFFERENT STRATEGIES WHEN VARYING THE SIZE OF THE ENERGY STORAGE.

		Energy performance				Network performance				
Energy storage size [kWh]	Strategy	Total energy consumed [kWh]	Total energy bought [kWh]	Time sufficient energy [%]	ΔP [%]	Average geometrical coverage [%]	Average user coverage [%]	Average network capacity [Mbps]	ΔU [%]	ΔC [%]
40	1: No action	2563	1510	32.7	—	85.1	97.3	452	—	—
	2: All off	1752	688	31.5	-54.4	86.5	95.3	226	-2.1	-50.0
	3: 1 to 4 off	1812	783	32.7	-48.1	85.0	95.6	240	-1.7	-46.9
80	1: No action	2574	1280	41.1	—	84.8	97.0	453	—	—
	2: All off	1901	605	41.7	-52.7	85.1	95.9	267	-1.1	-41.1
	3: 1 to 4 off	1930	634	42.3	-50.5	85.5	96.1	275	-0.9	-39.3
120	1: No action	2598	1236	44	—	85.5	97.1	457	—	—
	2: All off	1958	577	45.2	-53.3	85.1	95.8	281	-1.3	-38.5
	3: 1 to 4 off	1980	612	45.8	-50.5	85.4	96.2	288	-0.9	-37.1
160	1: No action	2529	1118	46.4	—	85.3	97.1	446	—	—
	2: All off	1978	547	47	-51.1	86.4	96.0	286	-1.1	-35.7
	3: 1 to 4 off	2001	590	45.8	-47.3	84.9	95.9	293	-1.2	-34.3

1) Energy bought: Fig. 7(a) shows the amount of energy bought as a function of the energy storage size. A larger energy storage clearly influences the amount of energy bought positively. Doubling the energy storage size

results in 12.7% less energy that should be bought when taking no action at all (1280 kWh for 80 kWh versus 1118 kWh for 160 kWh, Table III). A larger energy storage means of course that more (renewable) energy can be stored for future energy outages and thus reducing the amount of energy that should be bought from the traditional grid. This can also be seen from the time sufficient energy available parameter in Table III. For a storage size of 40 kWh, 32.7% of the time enough renewable energy is available to feed the network. When considering a storage size of 160 kWh, 46.4% of the time enough renewable energy is available.

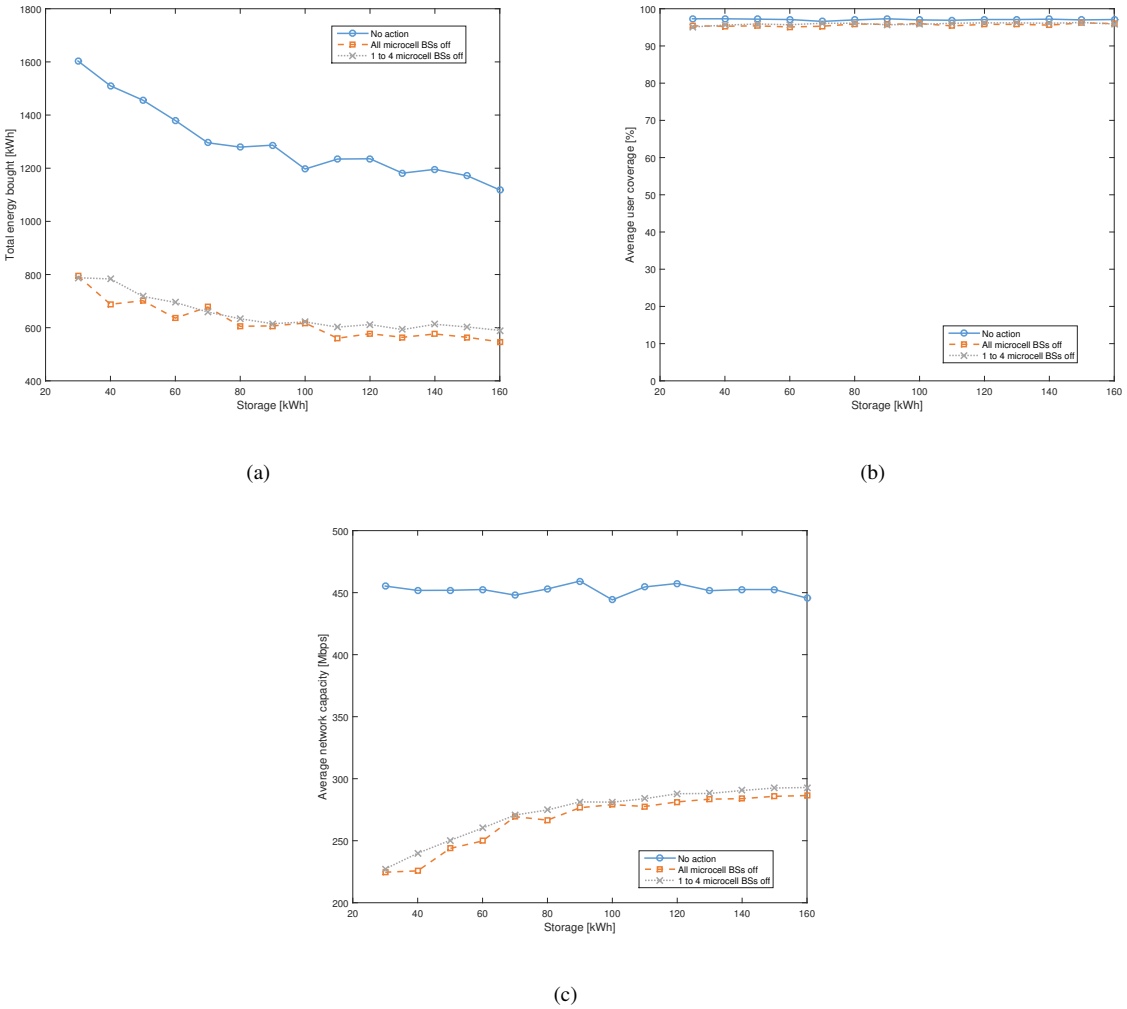

Fig. 7. Comparison of the amount of energy bought (a), the user coverage (b) and the network capacity (c) for the three different strategies as a function of the energy storage size.

The reduction in the amount of energy bought is a little bit lower when we switch off all the microcell base stations during an energy shortage. In this case, 9.6% less energy should be bought from the traditional grid when doubling the storage size (605 kWh for a size of 80 kWh versus 547 kWh for 160 kWh). The main reason is that less energy has to be bought as all microcell base stations are switched off (see Section III-B1). The lowest reduction is obtained by strategy 3. Increasing the storage size from 80 kWh to 160 kWh results in a reduction of 6.9%. The same reason as for the second strategy applies here, we have to buy less energy as we are turning off

base stations. However, strategy 3 keeps as much microcell base stations active as possible according to the amount of energy available, explaining this lower value.

Finally, Fig. 7(a) shows that the amount of energy bought stabilizes around 1180 kWh, 565 kWh, and 600 kWh, when applying strategy 1, 2, and 3, respectively, from an energy storage size of 110 kWh on (Table III). This is because the renewable energy produced by the PV modules is not high enough to completely fill the energy storage anymore.

2) Average user coverage: The influence of the energy storage size on the average user coverage is shown in Fig. 7(b). Similar to the PV model capacity (Section III-B2), the size of the energy storage has no influence on the performance of the "take no action" strategy. This is logical, as in this strategy, no base stations are shutdown and the shortage of power is just bought form the traditional grid.

For the two other strategies, the influence of the energy storage size on the user coverage is not very significant. When increasing the storage size from 30 kWh to 160 kWh, we only gain 1% of user coverage for both strategies. The more energy that can be saved, the more energy will become available for future shortages. We will have less moments where we have to switch off microcell base stations (see the time sufficient energy parameter in Table III) and thus more users can be covered.

3) Average network capacity: Fig. 7(c) shows the average network capacity as a function of the energy storage size. Again, it is noticed that an increasing storage size has no influence on this parameter when the first strategy is considered. The same reason applies here as for the relation between the average network capacity and the PV module capacity (Section III-B3). As no base stations are turned off, the network capacity does not change with varying energy storage size.

For the two other strategies, an improvement in network capacity is found when increasing the energy storage size. If we quadruple the storage size, the network capacity improves with 27.0% and 22.0% when applying the second and the third strategy, respectively (from 225.7 Mbps for 40 kWh to 286.6 Mbps for 160 kWh and from 239.9 Mbps to 292.9 Mbps respectively, Table III). As less energy is wasted due to the larger storage, more energy is available to feed the network during energy shortages. The moments, we have to turn off microcell base stations will be reduced (see also time sufficient energy parameter in Table III), thus resulting in a higher average network capacity.

Similar to the amount of energy bought (Section III-C1), Fig. 7(c) shows that the average network capacity stabilizes for energy storage sizes above 100 kWh as the PV modules do not produce enough renewable energy to fill the energy storage completely. For strategy 2, a network capacity of approximately 283 Mbps is obtained (Table III), while for strategy 3, a value of 288 Mbps is retrieved (Table III).

D. Influence of the time window on the energy and network performance

The last parameter we study is the time window. The following settings are assumed:

- – Capacity of the PV module: 100 kWp

– Capacity of the energy storage: 50 kWh
– Time window: varying from 1h to 10h in steps of 1h

All other parameters remain the same as in Section II-A. The amount of energy bought, the average user coverage, and the average network capacity are again considered as the three key parameters to evaluate and will be discussed in the following sections. Note that the performance of the different strategies is thoroughly investigated above and we refer therefore to Section III-B1, III-B2, III-B3. Table IV summarizes the absolute and relative values of the other energy and network performance parameters as well for 5 different time windows.

TABLE IV
ENERGY AND NETWORK PERFORMANCE OF THE DIFFERENT STRATEGIES WHEN VARYING THE TIME WINDOW.

		Energy performance				Network performance				
Time window [h]	Strategy	Total energy consumed [kWh]	Total energy bought [kWh]	Time sufficient energy [%]	ΔP [%]	Average geometrical coverage [%]	Average user coverage [%]	Average network capacity [Mbps]	ΔU [%]	ΔC [%]
1	1: No action	2525	1605	28	—	85.4	96.7	444	—	—
	2: All off	1699	756	28	-52.9	84.8	94.7	209	-2.1	-53.0
	3: 1 to 4 off	1724	797	28	-50.4	85.7	94.7	216	-1.9	-51.4
4	1: No action	2525	1605	28	—	85.4	96.7	444	—	—
	2: All off	1501	534	41.1	-66.8	85.4	94.2	155	-2.6	-65.0
	3: 1 to 4 off	1574	649	34.5	-59.6	85.7	94.2	176	-2.3	-60.3
6	1: No action	2525	1605	28	—	85.4	96.7	444	—	—
	2: All off	1329	442	45.2	-72.5	85.0	92.9	111	-3.9	-75.1
	3: 1 to 4 off	1462	525	42.9	-67.3	86.6	92.9	145	-2.8	-67.4
8	1: No action	2525	1605	28	—	85.4	96.7	444	—	—
	2: All off	1287	473	44	-70.5	85.0	93.1	92	-3.7	-79.4
	3: 1 to 4 off	1359	502	45.2	-68.8	85.6	93.1	114	-3.6	-74.2
10	1: No action	2525	1605	28	—	85.4	96.7	444	—	—
	2: All off	1280	474	44	-70.5	85.1	93.1	91	-3.7	-79.5
	3: 1 to 4 off	1335	531	44	-67.0	85.8	93.1	104	-3.0	-76.5

1) Energy bought: Fig. 8(a) shows the influence of a varying time window on the amount of energy bought from the traditional grid for the three different strategies. For the first strategy, the amount of energy bought does not depend at all on the considered time window. This is quite obvious. Even if we predict an energy shortage in the near future, we are not able to save any energy in advance as we do not turn any base stations off. For the two other strategies, a larger time frame results in general in a lower amount of energy bought as shown in Fig. 8(a)). For example, moving from a 1h to a 5h time window reduces the amount by 40.7% and 22.7% when using strategy 2 and 3, respectively (755.9 kWh and 796.7 kWh for 1h versus 448.2 kWh and 615.8 likWh for 5h, respectively, Table IV). The larger the used time window, the earlier we can start turning off base stations in case

an energy shortage is predicted, and the more energy can be saved in advance to cover the energy shortage.

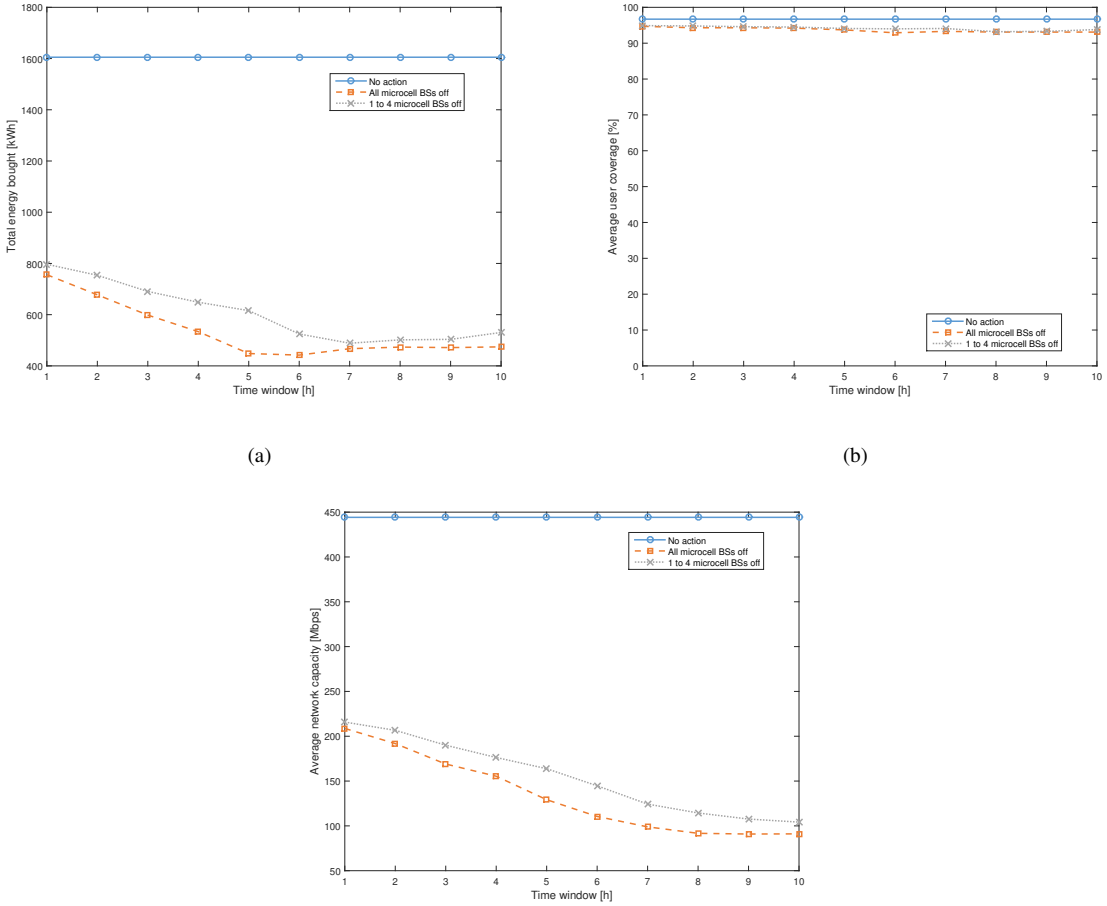

Fig. 8. Comparison of the amount of energy bought (a), the user coverage (b) and the network capacity (c) for the three different strategies as a function of the time window.

Note, however, that it is not useful to enlarge the time window endlessly (after a time window of 7 h). When all microcell base stations are switched off (strategy 2), the amount of energy that should be bought stabilizes for time window values higher or equal to 5h. Fig. 8(a). From this point on, we have to buy about 470 kWh (Table IV). Similarly, for the second strategy, the energy bought stabilizes from a value of 7h on (Fig. 8(a)): approximately 500 kWh of energy should be bought (Table IV). The reason is two-folded. First, considering a large time window always results in a positive prediction of an energy shortage in the future. Because of the positive prediction, base stations are switched off and we will never have a fully operational network. Second, the amount of energy that is saved can no longer be stored due to the limitation of the energy storage. The reason of the difference in time window (5h versus 7h, as mentioned above) between the two strategies is that for the third strategy, as much microcell base stations are kept running as possible, thus saving a little bit less energy than for the second strategy.

2) Average user coverage: Fig. 8(b) shows the average user coverage when varying the time window between 1h and 10h. Similar to the amount of energy bought, the time window has no influence on the user coverage performance for the reference scenario. In this way, it is not possible to save energy in advance, and thus the user coverage remains the same independent of the considered time window. Slightly less users (about 2%) are covered when considering the other two strategies. The more in advance an energy shortage is predicted, the more in advance base stations are shutdown. During these periods, the users need to be reconnected to the active base stations, which is unfortunately not always possible, resulting in a lower user coverage.

3) Average network capacity: The influence of the time window on the average network capacity is shown in Fig. 8(c). Once again, for strategy 1, no difference in average network capacity is noticed with a varying time window. As no base stations are turned off, there is no ability to save energy in advance and we just have to buy energy, keeping the network fully operational.

For the two other strategies, a decrease in the network capacity. When applying strategy 2, the network capacity is reduced by 56.4% for a 10h time window compared to a 1h time window (208.7 Mbps for 1h versus 91.1 Mbps for 10h, Table IV). The larger the time window, the more in advance the base stations are turned off and the more often we need to reconnect user which is not always possible. For strategy 3, a lower decrease of 51.7% is found (215.8 Mbps for 1h versus 104.2 Mbps for 10h, Table IV), because this strategy tries to keep as much microcell base stations active as possible. Purely from the network perspective, the first strategy i.e., no action at all, is the best (no 50% less in capacity) but in reality the networks with strategy 2 and 3 will save more energy.

For both strategy 2 and 3, the average network capacity stabilizes for time windows larger or equal than 7h (Fig. 8(c) & Table IV). The reason is two-folded. First, the larger the time window, the higher the chance there will be an energy shortage in this time frame and the more often base stations are turned off. If the time window becomes too large, we will always predict an energy shortage and never have a fully operational network. Second, we will not be able to store all the extra energy due to the limitation of the energy storage system.

E. Prediction models

In this section, we determine an analytical prediction model for the different relations discussed in the previous sections. These models can be used to investigate and predict the total energy bought, the average user coverage, and the average network capacity when developing an appropriate energy provisioning and storage system. The influence of the PV capacity, the energy storage, and the time window, can be evaluated individually by using the models presented in the first three sections below. A multiple regression model of all these parameters is available in the last subsection. As mentioned in Section II-A, 8 macrocell base stations are here considered.

1) Performance as a function of the PV capacity: The models obtained in this section are based on the assumptions and results presented in Section III-B. Table V shows the Pearson correlation (p-value) between the different network and energy performance parameters (total energy bought E_b, average user coverage C_U, and average network capacity C_n) and the PV capacity (C_{PV}) parameter for the three considered strategies. Only the statistical significant relations i.e., where a p-value equal or lower than 0.05, is found, will be modelled i.e., for

strategies 2 and 3 (Table V). Table V shows that no model will be available for C_{PV} versus C_n for strategy 1. As this strategy does not switch off microcell base stations, changing the PV capacity will have no influence on these two network performance parameters (Section III-B)

TABLE V

PEARSON CORRELATION (p-VALUE) FOR THE NETWORK AND ENERGY PERFORMANCE PARAMETERS AND THE DIFFERENT INPUT PARAMETERS (PV PANEL CAPACITY C_{PV}, ENERGY STORAGE SIZE S, AND TIME WINDOW T).

Input parameter	Strategy	Total energy bought E_b	Average user coverage C_U	Average network capacity C_n
PV panel capacity C_{PV}	1: No action	1.92e-06	0.26	0.54
	2: All off	2.77e-08	0.002	3.18e-05
	3: 1 to 4 off	2.52e-07	0.0001	4.33e-06
Energy storage size S	1: No action	1.81e-06	0.50	0.53
	2: All off	1.72e-05	0.004	6.78e-06
	3: 1 to 4 off	2.5e-05	0.006	1.98e-06
Time window T	1: No action	1.0	1.0	1.0
	2: All off	0.004	0.0003	8.18e-06
	3: 1 to 4 off	0.0002	0.0004	3.32e-08

Table VI presents the prediction models for the considered network and energy performance parameters based on the PV panel size. These models are obtained by OLS (Ordinary Linear Squares) regression for those relations that are considered to be statistical significant (Table V). Table VI shows that the total energy bought E_b is negatively linear related to the PV panel size C_{PV}. The larger the PV panel, the more renewable energy is produced, and the less energy that should be bought from the traditional grid. For all strategies, our models predict the total energy bought in at least 86% of the cases ($R^2 \geqslant 0.86$, Table VI). Furthermore, the absolute value of the standardized residual of none of our observations is higher or equal than 2. The average user coverage and the average network capacity are positively linear related to the PV panel size. The larger the PV panels, the more renewable energy is produced, the lower the occurences of energy shortages and thus the microcell base stations have to be switched off less frequently. Our models allow to predict the network performance correctly 72% of the time ($R^2 \geqslant 0.72$, Table VI), expect for the average user coverage when using the second strategy. However, also for the latter, the absolute value of the standardized residual of all of our observations is lower than 2.

2) Performance as a function of the energy storage: Here, the total energy bought E_b, the average user coverage C_u, and the average network capacity C_n is modelled as a function of the energy storage size S. To this end, the results proposed in Section III-C are used. Again for strategy 1, a p-value $\geqslant 0.05$ is obtained for C_u and $_n$ and will thus not be modelled (Table V).

The models for the energy and network performance parameters as a function of the energy storage size are listed in Table VI. The total energy bought E_b is negatively linear related to the energy storage size S. The larger the energy storage, the more renewable energy can be saved for future shortages and thus the less energy that should be bought. Conversely, the average user coverage and the average network capacity are positively linear related to the energy storage size. The larger the energy storage, the more energy can be saved for future shortages and the less often we have to turn off microcell base stations, resulting in a higher network performance. The models

TABLE VI

ANALYTICAL PREDICTION MODELS FOR THE NETWORK AND ENERGY PERFORMANCE PARAMETERS AS A FUNCTION OF THE PV PANEL CAPACITY C_{PV} (IN KWP), THE STORAGE SIZE S (IN KWH), AND THE TIME WINDOW T (IN H). $\hat{E}_b$, $\hat{C}_u$, AND $\hat{C}_n$ ARE THE ESTIMATE VALUES OF THE ENERGY BOUGHT, THE USER COVERAGE, AND THE NETWORK CAPACITY, RESPECTIVELY.

Input parameter	Strategy	Output parameter	Equation	R^2
PV panel capacity C_{PV} (in kWp)	1: No action	Total energy bought E_b (in kWh)	$\hat{E}_b$ = -3.5 C_{PV} + 2001.2	0.86
	2: All off	Total energy bought E_b (in kWh)	$\hat{E}_b$ = -1.3 C_{PV} + 903.5	0.93
		Average user coverage C_u (in %)	$\hat{C}_u$ = 0.01 C_{PV} + 93.8	0.57
		Average network capacity C_n (in Mbps)	$\hat{C}_n$ = 0.6 C_{PV} + 142.1	0.78
	3: 1 to 4 off	Total energy bought E_b (in kWh)	$\hat{E}_b$ = -1.1 C_{PV} + 899.2	0.90
		Average user coverage C_u (in %)	$\hat{C}_u$ = 0.01 C_{PV} + 93.6	0.72
		Average network capacity C_n (in Mbps)	$\hat{C}_n$ = 0.7 C_{PV} +142.8	0.84
Energy storage size S (in kWh)	1: No action	Total energy bought E_b (in kWh)	$\hat{E}_b$ = -3.1 S + 1594.2	0.86
	2: All off	Total energy bought E_b (in kWh)	$\hat{E}_b$ = -1.5 S + 765.5	0.80
		Average user coverage C_u (in %)	$\hat{C}_u$ = 0.006 S + 95.1	0.51
		Average network capacity C_n (in Mbps)	$\hat{C}_n$ = 0.5 S + 221.7	0.83
	3: 1 to 4 off	Total energy bought E_b (in kWh)	$\hat{E}_b$ = -1.4 S + 788.5	0.79
		Average user coverage C_u (in %)	$\hat{C}_u$ = 0.006 S + 95.4	0.48
		Average network capacity C_n (in Mbps)	$\hat{C}_n$ = 0.5 S + 229.1	0.86
Time window T (in h)	1: All off	Total energy bought E_b (in kWh)	$\hat{E}_b$ = -29.1 T + 694.4	0.66
		Average user coverage C_u (in %)	$\hat{C}_u$ = -0.2 T + 94.7	0.82
		Average network capacity C_n (in Mbps)	$\hat{C}_n$ = -14.2 T + 211.7	0.93
	2: 1 to 4 off	Total energy bought E_b (in kWh)	$\hat{E}_b$ = -34.3 T + 794.2	0.85
		Average user coverage C_u (in %)	$\hat{C}_u$ = -0.2 T + 95.1	0.81
		Average network capacity C_n (in Mbps)	$\hat{C}_n$ = -13.6 T + 229.8	0.98
PV panel capacity C_{PV} (in kWp) Energy storage size S (in kWh) Time window T (in h)	1: No action	Total energy bought E_b (in kWh)	$\hat{E}_b$ = -3.5 C_{PV} - 3.7 S + 2162.6	0.92
		Average user coverage C_u (in %)	$\hat{C}_u$ = 0.04 C_{PV} - 1.4 T + 91.1	0.70
		Average network capacity C_n (in Mbps)	$\hat{C}_n$ = -0.8 T + 448.4	0.32
	2: All off	Total energy bought E_b (in kWh)	$\hat{E}_b$ = -1.0 C_{PV} - 1.6 S - 41.1 T + 962.7	0.82
		Average user coverage C_u (in %)	$\hat{C}_u$ = 0.01 C_{PV} + 0.008 S - 0.2 T + 93.5	0.90
		Average network capacity C_n (in Mbps)	$\hat{C}_n$ = 0.7 C_{PV} + 0.6 S - 15.6 T + 122.6	0.90
	3: 1 to 4 off	Total energy bought E_b (in kWh)	$\hat{E}_b$ = -1.1 C_{PV} - 1.6 S - 36.7 T + 962.7	0.89
		Average user coverage C_u (in %)	$\hat{C}_u$ = 0.01 C_{PV} + 0.008 S - 0.2 T +93.4	0.89
		Average network capacity C_n (in Mbps)	$\hat{C}_n$ = 0.7 C_{PV} + 0.6 S - 13.4 T + 130.6	0.97

predict the total energy bought and the average network capacity correctly in more than 80% of the cases ($R^2 \geqslant 0.8$) and we have no standarized residuals with an absolute value $\geqslant 2$. The average user coverage has a lower R^2 of approximately 0.5. This is due to 1 outliner in the observations, which has a standardized residual with an absolute value of more than 2 (but less than 2.5).

3) Performance as a function of the time window: To determine the models as a function of the time window T, the results and assumptions from Section III-D are considered. Table V shows the correlation between the different performance parameters and the time window. When applying the first strategy, none of the parameters is statistically signicant (p-value $\geqslant 0.5$) because this strategy just buys energy and does not turn off any base stations. No models will thus be proposed for the first strategy.

The prediction models as a function of the time window T for the other strategies are shown in Table VI. The total energy bought E_b, the average user coverage C_u, and the average network capacity C_n are all negatively related to the time window. A larger time window results on the one hand in more energy that can be saved in advance, so less energy should be bought. On the other hand, the microcell base stations will be switched off more frequently, thus a lower network performance is obtained. The models are reliable as R^2 values between 0.66 and 0.98 are obtained and none of the observations has a residual of more than 2 standard deviations.

4) Performance as a function of multiple parameters: A drawback of the models proposed above is that they only allow to predict the energy and network performance based on one parameter. However, when one is varying the energy storage size, one might also be interested in varying the PV panel size or the time window. In this section, we propose a multiple regression model for the different strategies and the different energy and network performance parameters as a function of the PV panel capacity C_{PV}, the energy storage size S, and the time window T. To this end, we combined all the results obtained in Sections III-B, III-C, and III-D. Table VI presents the different prediction models. Note that not all parameters C_{PV}, S, and T occur in each model. Whenever a parameter turns out to be not statistical significant for the multiple regression model (p - value $\geqslant 0.05$), the parameter was removed from the model. All our models provide reliable predictions for the energy and network performance parameter (R^2 between 0.7 and 0.92), except for the average network capacity when applying strategy 1. In this case, the model only predicts the average network capacity correctly in 32% of the cases.

Let us now consider a practical example of use of the fitted expressions to derive actual values for the (in hours) system parameters. We would like to derive a proper combination of PV panel size and storage capacity and select the most appropriate policy, assuming that a constraint exists on the minimum average user coverage C_u to be guaranteed. Let us assume a target of $C_u \geqslant 95\%$ and a window size either of 1h or 10h. Furthermore, our sample scenario shows some spacial limitations, hence the area covered by PV panels should be limited as much as possible. When strategy 1 is applied, the following inequalities hold:

$$C_{PV} \geqslant 132.5 \text{ [kWp]}, \quad \text{for T = 1h}$$
$$C_{PV} \geqslant 447.5 \text{ [kWp]}, \quad \text{for T = 10h}$$

For T=10h, the adoption of strategy 1 is clearly unfeasible, due to the large surface required by a PV system whose capacity is 447.5 kWp. Setting a lower T, a smaller S_{PV} is required, still rather huge. Let us then consider the other 2 strategies. In case strategy 2 is applied, these expressions hold:

$$C_{PV} \geqslant (-0.8\ S + 170) \text{ [kWp]}, \quad \text{for T = 1h}$$
$$C_{PV} \geqslant (-0.8\ S + 350) \text{ [kWp]}, \quad \text{for T = 10h}$$

In this case, C_{PV} can be limited by selecting a battery whose size is for example at least 70 kWh, in case of T = 1h. In case of T = 10h, larger S is needed to limit C_{PV} to reasonable values. Similar inequalities hold for the third strategy:

$$C_{PV} \geqslant (-0.8\ S + 180)\ \text{[kWp]},\quad \text{for T = 1h}$$
$$C_{PV} \geqslant (-0.8\ S + 360)\ \text{[kWp]},\quad \text{for T = 10h}$$

In our example, since we do not have constraints either on the maximum energy bought from the grid or on the minimum average network capacity, we can privilege the reduction of C_{PV}. Strategy 1 should hence be excluded, since a huge C_{PV} would be required even with a small window T. Among the other two strategies, the second one, with the window T set to 1h, allows to obtain the smallest C_{PV} at the price of a lower increase in the battery size S. Indeed, when C_{PV} is decreased, a larger energy storage is required. A battery of 70 kWh combined with a PV system of 114 kWp assure that less than 5% of users on average will experience a lack of network coverage. To further shrink the PV system size, it will be enough to envision a larger battery set.

F. General guidelines

In this section, we give general advice on the most applicable strategy and the most optimal settings for the energy system based on the study above.

The choice between the three strategies depends on the objective parameter. If network performance is highly important, the "no action at all" strategy (strategy 1) is obviously the best (more than 96% user coverage and no loss of 50% network capacity). If the focus is on the energy performance, we suggest to use the second strategy "all microcell base stations off" (approximately 50% less energy should be bought). A trade-off between energy and network performance is offered by the third strategy "1 to 4 microcell base stations off". In general, our results show that both the turning off strategies are very useful when one wants to reduce the amount of (non-renewable) energy that should be bought from the power grid, despite the reduction in network performance. However, this reduction in network performance is still acceptable as mostly a user coverage above 95% is obtained. Furthermore, we recommend to use a time window when the energy performance is the key parameter.

For the settings of the energy production and storage system and the scenario here considered, we recommend to use the following values:

- – Capacity PV module: 100 kWp
  – Size energy storage: 50 kWh (80 kWh at most)
  – Time window: 5h

We refer to Sections III-B, III-C, and III-D, respectively, for the discussion of these appropriate values.

IV. Conclusion

Due to the possible future depletion, the increasing energy cost, and the effect on the climate change of burning fossil fuels, the use of renewable energy sources has started to enter the market during the last decade. Wireless access networks are currently large energy consumers and in the future they will become part of the smart grid which will be completely off-grid powered by renewables. However, these renewable energy sources do not provide the same supply continuity as fossil fuels. Therefore, it is important to introduce an energy-aware management system of the radio resources available in the mobile network. In this study, we propose such an energy-aware

management system. The goal of these strategies is to limit the amount of energy that should be bought from the power grid. Three different strategies are compared for a realistic small-scale LTE outdoor network powered by solar energy and the traditional power grid. Furthermore, the influence of a time window, applying a strategy in advance to save energy for a future predicted energy shortage, is studied.

In general, using an energy-aware strategy is very useful since it will reduce the network's power consumption significantly (between 21% and 41% depending on the considered strategy and settings of the energy production and storage system) during a solar energy shortage. Because of this, even up to 56% less energy should be bought from the traditional grid by switching off microcell base stations. This results of course in a loss of network performance: between 34% to 65% less capacity is offered by the network. However, the overall user coverage is still acceptable (more than 94%). Introducing a time window can further reduce the amount of energy bought: up to 19% less energy should be bought when using a 5h time window. The offered network capacity will unfortunaltey also be further decreased (even up to 80%), but most users are still covered (more than 93%).

The choice for a certain strategy depends on the considered objective. If the network performance is the most important parameter, we recommend to keep the network fully operational and just buy the needed energy. When the energy performance is the key parameter, we recommend to use the strategy switching off all microcell base stations during an energy shortage combined with a time window of more than 1h. A trade-off between energy and network performance is provided by the strategy switching off microcell base stations gradually depending on the amount of energy that should be bought.

Based on a thorough analysis of the different parameters of the energy production and storage system, we recommmend to use a capacity of 100 kWp for the PV modules, an energy storage of 50 kWh (no more than 80 kWh) and a time window of 5h for the considered scenario. Furthermore, prediction models for the energy and network performance parameters as a function of the PV panel capacity, the energy storage size, and the time window (individually and jointly) are proposed for the different strategies. Future research will consist of investigating the influence of the energy management policies on a large scale, implementing more advanced strategies accounting for (energy) cost, and considering other types of renewable energy sources as well.

ACKNOWLEDGMENT

Margot Deruyck is a Post-Doctoral fellow of the FWO-V (Research Foundation - Flanders, Belgium) and received a travel grant from FWO-V to perform research at the Politecnico di Torino.

REFERENCES

[1] S. Lambert, M. Deruyck, W. Van Heddeghem, B. Lannoo, W. Joseph, D. Colle, M. Pickavet, P. Demeester, *Post-peak ICT: Graceful degradation for communication networks in an energy constrained future*, IEEE Communications Magazine, Vol. 53, No. 11, pp. 166-174, 2015.

[2] M. Etoh, T. Ohya, Y. Nakayama, *Energy Consumption Issues on Mobile Network Systems*, International Symposium on Applications and the Internet (SAINT), pp. 365-368, 2008.

[3] MA. Imran,E. Katranaras, G. Auer, O. Blume, V. Giannini, I. Godor, Y. Jading, M. Olsson, D. Sabella, P. Skillermark, and others, *Energy efficiency analysis of the reference systems, areas of improvements and target breakdown*, Tech. Rep. ICT-EARTH deliverable, 2011.

[4] H. Al Haj Hassan, L. Nuyami, A. Pelov, *Renewable energy in cellular networks:a survey*, IEEE Online Conference on Green Communications (GreenCom), pp. 1-7, 2013.

[5] M.A. Marsan, G. Bucalo, A. Di Caro, M. Meo, Y. Zhang, *Towards zero grid electricity networking: Powering BSs with renewable energy sources*, IEEE International Conference on Communications Workshops (ICC), pp. 596-601, 2013.

[6] M.A. Marsan, R. Gerboni, J.G. Iglesias, M. Meo, Y. Zhang, "Optimizing the Power Supply of a Macro BS Connected to a PV Panel and the Power Grid", GTTI meeting (Gruppo Telecommunicazioni e Tecnologie dell'Informazione, 2014.

[7] M. Meo, Y. Zhang, R. Gerboni, M.A. Marsan, "Dimensioning the power supply of a LTE macro BS connected to a PV panel and the power grid", IEEE International Conference on Communications (ICC), pp. 178-184, 2015.

[8] H. Toa, N. Ansari, *On Optimizing Green Energy Utilization for Cellular Networks with Hybrid Energy Supplies*, IEEE Transactions on Wireless Communications, Vol. 12, No. 8, pp. 3872-3882, 2013.

[9] X. Fang, S. Misra, G. Xue, D. Yang, *Smart Grid - The New and Improved Power Grid: A Survey*, IEEE Communications Surveys & Tutorials, Vol. 14, No. 4, pp. 944-980, 2012.

[10] M.S. Obaidat, A. Anpalagan, I. Woungang, *Handbook of Green Information and Communication Systems*, Academic Press, 2013, ISBN: 978-0-1241-5844-3.

[11] H. Ghazzai, E. Yaacoub, M.-S. Alouini, A. Abu-Dayya, *Optimized green operation of LTE networks in presence of multiple electricity providers*, IEEE Globecom Workshops (GC Wkshps), pp. 664-669, 2012.

[12] H. Ghazzai, E. Yaacoub, M.-S. Alouini, A. Abu-Dayya, *Performance of Green LTE Networks Powered by the Smart Grid with Time Varying User Density*, 78th IEEE Vehicular Technology Conference (VTC Fall), pp. 1-6, 2013.

[13] J. Wu, Y. Zhang, M. Zukerman, and E. K. N. Yung, "Energy-efficient base-stations sleep-mode techniques in green cellular networks: A survey," *IEEE Communications Surveys Tutorials*, vol. 17, no. 2, pp. 803–826, Secondquarter 2015.

[14] S. Zhou, J. Gong, and Z. Niu, "Sleep control for base stations powered by heterogeneous energy sources," in *2013 International Conference on ICT Convergence (ICTC)*, Oct 2013, pp. 666–670.

[15] H. Xu, T. Zhang, Z. Zeng, and D. Liu, "Joint base station operation and user association in cloud based hcns with hybrid energy sources," in *2015 IEEE 26th Annual International Symposium on Personal, Indoor, and Mobile Radio Communications (PIMRC)*, Aug 2015, pp. 2369–2373.

[16] M. Dalmasso, M. Meo, and D. Renga, "Radio resource management for improving energy self-sufficiency of green mobile networks," in *Performance Evaluation Review*, vol. 44, no. 2, 2016, pp. 82–87.

[17] H. Ghazzai, M. J. Farooq, A. Alsharoa, E. Yaacoub, A. Kadri, and M. S. Alouini, "Green networking in cellular hetnets: A unified radio resource management framework with base station on/off switching," *IEEE Transactions on Vehicular Technology*, vol. PP, no. 99, pp. 1–1, 2016.

[18] Y. L. Che, L. Duan, and R. Zhang, "Dynamic Base Station Operation in Large-Scale Green Cellular Networks," *IEEE Journal on Selected Areas in Communications*, 34(12):3127–3141, Dec 2016.

[19] M. Deruyck, W. Joseph, E. Tanghe, and L. Martens, "Reducing the power consumption in LTE-Advanced wireless access networks by a capacity based deployment tool," *Radio Science*, 49(9):777–787, 2014.

[20] http://pvwatts.nrel.gov/pvwatts.php, last accessed: February 2015.

[21] M. Deruyck, E. Tanghe, D. Plets, L. Martens, W. Joseph, *Optimizing LTE wireless access networks towards power consumption and electromagnetic exposure of human beings*, Elsevier Computer Networks, Vol. 94, pp. 29-40, 2016.

[22] M. Deruyck, W. Joseph, L. Martens, *Power consumption model for macrocell and microcell base stations*, Transactions on Emerging Telecommunications Technologies, Vol. 25, No. 3, pp. 320-333, 2014.

[23] Yi Zhang, Ł. Budzisz, M. Meo, A. Conte, I. Haratcherev, G. Koutitas, L. Tassiulas, M. A. Marsan, and S. Lambert, *An overview of energy-efficient base station management techniques*,2013 24th Tyrrhenian International Workshop on Digital Communications - Green ICT (TIWDC), pp. 1-6, Sept 2013.

[24] Ł. Budzisz, F. Ganji, G. Rizzo, M. Ajmone Marsan, M. Meo, Y. Zhang, G. Koutitas, L. Tassiulas, S. Lambert, B. Lannoo, M. Pickavet, A. Conte, I. Haratcherev, and A. Wolisz, *Dynamic resource provisioning for energy efficiency in wireless access networks: A survey and an outlook*, IEEE Communications Surveys Tutorials, 16(4):2259-2285, Fourthquarter 2014.

[25] D. Renga and M. Meo, *Modeling renewable energy production for base stations power supply*, 2016 IEEE International Conference on Smart Grid Communications (SmartGridComm), pp. 716-722, Nov 2016.

[26] A. P. Dobos, *PVWatts Version 5 Manual*, Sep 2014.

[27] H. Huang, J. Xu, Z. Peng, S. Yoo, D. Yu, D. Huang, and H. Qin, *Cloud motion estimation for short term solar irradiation prediction*, 2013 IEEE International Conference on Smart Grid Communications (SmartGridComm), pp. 696-701, Oct 2013.

[28] R. J. Bessa, A. Trindade, and V. Miranda, *Spatial-temporal solar power forecasting for smart grids*, IEEE Transactions on Industrial Informatics, 11(1):232-241, Feb 2015.

[29] S. A. Fatemi and A. Kuh, *Solar radiation forecasting using zenith angle*, 2013 IEEE Global Conference on Signal and Information Processing, pp. 523-526, Dec 2013.

[30] L. Ciabattoni, M. Grisostomi, G. Ippoliti, S. Longhi, and E. Mainardi, *On line solar irradiation forecasting by minimal resource allocating networks*, 2012 20th Mediterranean Conference on Control Automation (MED), pp. 1506-1511, July 2012.

[31] J. Shi, W. J. Lee, Y. Liu, Y. Yang, and P. Wang, *Forecasting power output of photovoltaic systems based on weather classification and support vector machines*, IEEE Transactions on Industry Applications, 48(3):1064-1069, May 2012.

[32] H. T. Yang, C. M. Huang, Y. C. Huang, and Y. S. Pai, *A weather-based hybrid method for 1-day ahead hourly forecasting of pv power output*, IEEE Transactions on Sustainable Energy, 5(3):917-926, July 2014.

[33] M. Deruyck, W. Joseph, B. Lannoo, D. Colle, L. Martens, *Designing Energy-Efficient Wireless Access Networks: LTE and LTE-Advanced*, Vol.17, No. 5, 2013, pp.39-45.

[34] M. Deruyck, E. Tanghe, W. Joseph, L. Martens, *Characterization and optimization of the power consumption in wireless access networks by taking daily traffic variations into account*, Eurasip Journal on Wireless Communications and Networking, pp. 1-12, 2012, doi: 10.1186/1687-1499-2012-248.

Margot Deruyck was born in Kortrijk, Belgium, on July 14, 1985. She received the M. Sc. degree in Computer Science Engineering and the Ph. D. degree from Ghent University, Ghent, Belgium, in 2009 and 2015, respectively. From September 2009 to January 2015, she was a Research Assistant with Ghent University - IMEC - WAVES (Wireless, Acoustics, Environment & Expert Systems - Department of Information Technology). Her scientific work is focused on green wireless access networks with minimal power consumption and minimal exposure from human beings. This work led to the Ph.D. degree. Since January 2015, she has been a Postdoctoral Researcher at the same institution where she continues her work in green wireless access network. Since October 2016, she is a Post-Doctoral Fellow of the FWO-V (Research Foundation - Flanders).

Daniela Renga is a Ph.D. student in Electrical, Electronics and Communications Engineering at the Politecnico di Torino, Italy. She received the Master degree in Computer and Communication Networks Engineering in 2014 from the Politecnico di Torino. In 2004 she received a Laurea degree in Medicine from the Università degli Studi di Torino, Italy. Her research interests are in the fields of energy efficient wireless networks, resource management, network modeling, smart grids and renewable energy sources for sustainable mobile networks.

Michela Meo received the Laurea degree in Electronic Engineering in 1993, and the Ph.D. degree in Electronic and Telecommunications Engineering in 1997, both from the Politecnico di Torino, Italy. Since November 2006, she is professor at the Politecnico di Torino. She co-authored about 200 papers and edited a book with Wiley and special issues of international journals, including ACM Monet, Performance Evaluation, and Computer Networks. She chairs the Steering Committee of IEEE OnlineGreenComm and the International Advisory Council of ITC. She is associate editor of IEEE Communications Surveys & Tutorials, area editor of IEEE Transactions on Green Communications and Networking, and was associate editor of IEEE Transactions of Networking. She was program co-chair of several conferences among which ACM MSWiM, IEEE Online GreenComm, IEEE ISCC, IEEE Infocom Miniconference, ITC. Her research interests include performance evaluation and modeling, green networking and traffic classification and characterization.

Luc Martens (M'92) received the M.Sc. degree in electrical engineering and the Ph.D. degree from Ghent University, Ghent, Belgium, in 1986 and 1990, respectively. From September 1986 to December 1990, he was a Research Assistant with the Department of Information Technology (INTEC), Ghent University. During this period, his scientific work was focused on the physical aspects of hyperthermic cancer therapy. His research work dealt with electromagnetic and thermal modeling and with the development of measurement systems for that application. This work led to the Ph.D. degree. Since 1991, he has been managing the Wireless & Cable research group at INTEC, which has been part of the iMinds Institute since 2004. Since April 1993, he has been also a Professor at Ghent University. He has authored or coauthored over 300 publications in the domain of electromagnetic channel predictions, dosimetry, exposure systems, and health and wireless communications. His experience and current interests are in modeling and measurement of electromagnetic channels, of electromagnetic exposure, e.g., around telecommunication networks and systems such as cellular base station antennas, and of energy consumption in wireless networks.

Wout Joseph (M'05-SM'12) was born in Ostend, Belgium, on October 21, 1977. He received the M. Sc. degree in electrical engineering and the Ph.D. degree from Ghent University (UGent), Ghent, Belgium, in 2000 and 2005, respectively. From September 2000 to March 2005, he was a Research Assistant with the iMinds/UGent-INTEC (Ghent University - Department of Information Technology). During this period, his scientific work was focused on electromagnetic exposure assessment. His research work dealt with measuring and modeling of electromagnetic fields around base stations for mobile communications related to the health effects of the exposure to electromagnetic radiation. This work led to the Ph.D. degree. Since April 2005, he has been a Postdoctoral Researcher with iMinds-UGent/INTEC. From October 2007 to October 2013, he was a Postdoctoral Fellow of Research Foundation- Flanders (FWO-V). Since October 2009, he has been a Professor in the domain of experimental characterization of wireless communication systems. His professional interests are electromagnetic field exposure assessment, propagation for wireless communication systems, antennas, and calibration. Furthermore, he specializes in wireless performance analysis and quality of experience.